Morphological Characteristics and Geochemical Indicators of Weathering in Gypsiferous Soils under Arid and Semi-Arid Conditions in Al-Shirqat District, Central Iraq

Ahmed Majeed Heeshan[1], Ayad Abdullah Khalaf [2]
[1]Department of Soil Sciences and Water Recourses, College of Agriculture, Tikrit University, Iraq
[2]Department of Soil Sciences and Water Recourses, College of Agriculture, Tikrit University, Iraq
*Corresponding author's email. ahmedmajeed@st.tu.edu.iq
https://orcid.org/0000-0002-1281-7654
https://orcid.org/0000-0002-5183-3999

Abstract

This study investigates the micromorphological and geochemical indicators of weathering in gypsum soils under arid and semi-arid conditions. Physical, chemical, geochemical, and microscopic results show that the soils in the studied sections develop under arid to semi-arid climatic conditions, with a clear predominance of secondary gypsum and calcium carbonate deposits. Chemical analyses revealed high gypsum content in several horizons, reaching a maximum of 847.84 $g.kg^{-1}$, accompanied by high SO_3 and CaO values, confirming the gypsum nature of many sections, particularly in the P3, P_5, P_7. The main oxides also showed variation in SiO_2 (9.60–55.27%), reflecting the difference in parent material between the silicate sedimentary and calcareous-gypsum sections. Weathering Indicators (CIA, CIW, PIA) indicated a general decrease in chemical weathering intensity, with average values not exceeding 35–37 in most sections, suggesting limited feldspar decomposition and weak leaching. In contrast, WIP, ICV, and WR Indicators recorded relatively high values, reflecting the relative freshness of the parent material, the predominance of primary minerals, and a high content of soluble basics, consistent with a low-leaching depositional environment. Thin-section results supported these conclusions, revealing an abundance of gypsum crystals in lenticular, needle-like, and sugar-like forms, varying in size from fine to very coarse, and the presence of incompletely oriented crystals due to dissolution and redeposition processes. Dissolution porosity (Po) resulting from gypsum dissolution, calcareous nodules, and a complex microstructure combining a subangular block structure and a granular structure were also observed. The presence of albite twinning in plagioclase feldspar indicates an igneous origin of the parent material with a low to moderate degree of weathering.

Keywords: Gypsum soils, chemical weathering indicators, micromorphology, major oxides, arid and semi-arid climate.

Introduction

Micromorphology is the microscopic study of oriented and undisturbed soil samples to determine the composition and spatial relationships of these components, with the aim of inferring genetic and temporal correlations **[1]**. **[2]**noted that the study of micromorphological properties of soils at the microscopic level is a modern field within soil science, useful for evaluating soil minerals, origin, formation processes, and geomorphological shaping. **[3]** demonstrated the use of microscopic soil morphology studies to analyze soil origin and evolution. Micromorphological studies indicate the presence of a calcite horizon and various accumulations, such as calcite needles and calcite nodules, in the Bk horizons **[4]**. Vughy, channel, and massive microstructures were found, with the b-fabric structure being predominantly crystalline, in the saline-sodic soils west of Lake Urmia **[5]**. Clay and salt cutans were also found in the studied soils. Calcium carbonate and salts were found as pore fillers, in addition to their crystallization

ISSN 2072-3857

within the soil. **[6]** studied the micromorphological properties of soils along the climotopo sequence in Kerman Province, central Iran, and confirmed that gypsum dissolution led to high gypsum accumulation within the pores of aridisols. **[7]**investigated the micromorphology of saline-gypsum soils in the Kheirabad and Sirjan regions, observing the presence of euhedral gypsum crystals and calcareous coverings in the gypsic and calcic horizons of the sabkha geomorphological site. The results of a micromorphological study of clay and calcareous horizons in soils of northern Iraq, conducted by **[8]**, showed the presence of discontinuous clay bands interspersed with iron oxides around or within the pores of soil particles in Erbil Province. The results of the morphological field description also confirmed this. Microscopic studies of some soil profiles in Baiji, central Iraq, along with laboratory analysis results, revealed the presence of gypsan and calcitan coverings, confirming the soil's exposure to original depositional sources originating from the Makhoul Mountains, which influenced the soil formation in the study area **[9]**. Similarly, the results of micromorphological characterization of salt-affected soils in the Al-Najmi Agricultural Project in Al-Muthanna Governorate, southern Iraq, confirmed various features related to microstructure and porosity, as well as coverings such as saline (silwan) and calcitan coverings. Calcitan coverings were found in all samples due to the soil formation characteristics of arid and semi-arid regions**[10]**. **[11]** studied the micromorphological characterization of salt-affected soils in the Middle Mesopotamian Plain and confirmed the presence of calcitan coverings. Salwans are the salt layers studied in thin- section studies. Numerous studies have investigated the impact of soil salinity on soil properties and plant growth **[12]**. Researchers have also characterized the salic, calcic, and gypsic horizons in soils of arid and semi-arid regions **[13]**. **[14]** demonstrated that studying the micromorphological structures of gypsum-containing soils contributes to understanding soil inheritance and evolution. They showed that soils containing lenticular gypsum crystals indicate a well-developed soil, while soils containing prismatic, platy, and columnar gypsum crystals indicate an underdeveloped soil. Similarly, **[15]** concluded during Their study of the micromorphological evidence of the development of calcareous soils in arid and semi-arid regions to the emergence of the argillic clay horizon, which is strongly related to free iron oxides, color index, transported clay index, and smectite/chloride + illite ratio. Total oxides represent the chemical analyses of oxides resulting from rock weathering. Total oxides are mobile and redistributed during weathering due to the decomposition of minerals **[16] [17] [18] [19]**. The redistribution and mobility of tellurium oxides in the secondary environment is a common method for determining the degree of weathering and the behavior of oxides during weathering (Beyala et al., 2009). Mobile total oxides with more diverse geochemical compositions (such as MgO, Na_2O, K_2O, and CaO) typically decrease with increasing weathering as they are released from host minerals and leached from the parent rock. Al_2O_3 , SiO_2 , MnO, P_2O_5 , TiO_2 and FeO are among the less common mobile and immobile oxides **[20] [21]**. **[22]** in their study of chemical weathering rates and mineralogical geochemical properties of soils, indicated that the use of chemical weathering Indicators is important for understanding soil evolution characteristics. These Indicators include CIA, CIW, Base/R2O3, WIP, and PIA. The results clearly showed that topographic conditions significantly influence the physical, chemical, mineralogical, and morphological

ISSN 2072-3857

properties of soils, both directly and indirectly, in the region. The Chemical Change Index (CIA) is used as a prime example in India for assessing soil composition **[23]**. Triple ACN-K and A-CNK-FM schemes were developed to determine the degree of soil weathering in the Mahi catchment, Gujarat, and documented the dominance of smectite minerals in semi-arid, water-scarce areas (Sharma et al., 2013). Various geochemical Indicators are used to assess the weak to moderate weathering of ancient soil deposits in the Karua Basin of the Kashmir Valley (Chandra et al., 2016).

This study aims to evaluate soil weathering processes in gypsiferous soils under arid and semi-arid conditions in Al-Shirqat District, Iraq, by analyzing major oxides and calculating chemical weathering indices. The study also seeks to assess the vertical variation of these properties within soil pedons and to understand their relationship with soil development and pedogenic processes.

Material and Methods

2.1 Study Area

Seven representative Pedons (P_1, P_2, P_3, P_4, P_5, P_6, P_7). were selected from different locations in Al-Shirqat District, Salah ad-Din Governorate, central Iraq, to study the micromorphological and geochemical properties of gypsum soils under arid and semi-arid climatic conditions Figure 1. The study area lies within an arid to semi-arid climatic zone characterized by low annual rainfall and high evapotranspiration rates, creating favorable conditions for the accumulation of salts and gypsum in the soil profile.

Most of the soils in the study area belong to the Aridisols order according to the American Soil Taxonomy. These soils are formed in arid environments characterized by weak leaching processes and the accumulation of salts, sulfates, and carbonates in the subsurface horizons. The seven Pedons were chosen to represent the variation in geomorphological locations, parent material, and degree of pedogenic development within Al-Shirqat District, where gypsum-rich sedimentary deposits are widespread. The studied Pedons were assigned the codes (P_1, P_2, P_3, P_4, P_5, P_6, P_7). Each Pedon was morphologically described in the field according to the approved soil description manual, with genetic horizons identified and representative samples taken from each horizon for physicochemical and mineralogical analyses (XRD, XRF). Micromorphological characteristics were also studied through thin-section preparation and microscopic examination. The geographic coordinates of each pedon were recorded using GPS, and their locations are shown in Table 1.

2.2 Climate

Al-Shirqat District, Salah Al-Din Governorate, is characterized by an arid to semi-arid continental climate. The mean annual temperature ranges from 19–23 °C, with hot summers (often exceeding 40 °C) and cool winters. The average annual rainfall is approximately 250–350 mm, concentrated mainly between November and March, while summers are almost completely dry. These climatic conditions promote limited leaching and favor the accumulation of gypsum and soluble salts within the soil profile.

2.3 Field work

Soil Pedons were dug at the selected sites mentioned above. Then, disturbed and undisturbed soil samples were taken from the existing horizons, and morphology was described according to the method described by the studies **[24]**, **[25]**. The samples were then transported to the laboratory for the necessary analyses.

ISSN 2072-3857

2.4 Physical and chemical properties

Soil samples were collected from the field and transported to the laboratory for analysis. Disturbed samples were air-dried, gently crushed, and sieved through a 2-mm mesh. Physical and chemical analyses were conducted following standard procedures. Particle size distribution was determined using the hydrometer method **[26].** Soil pH

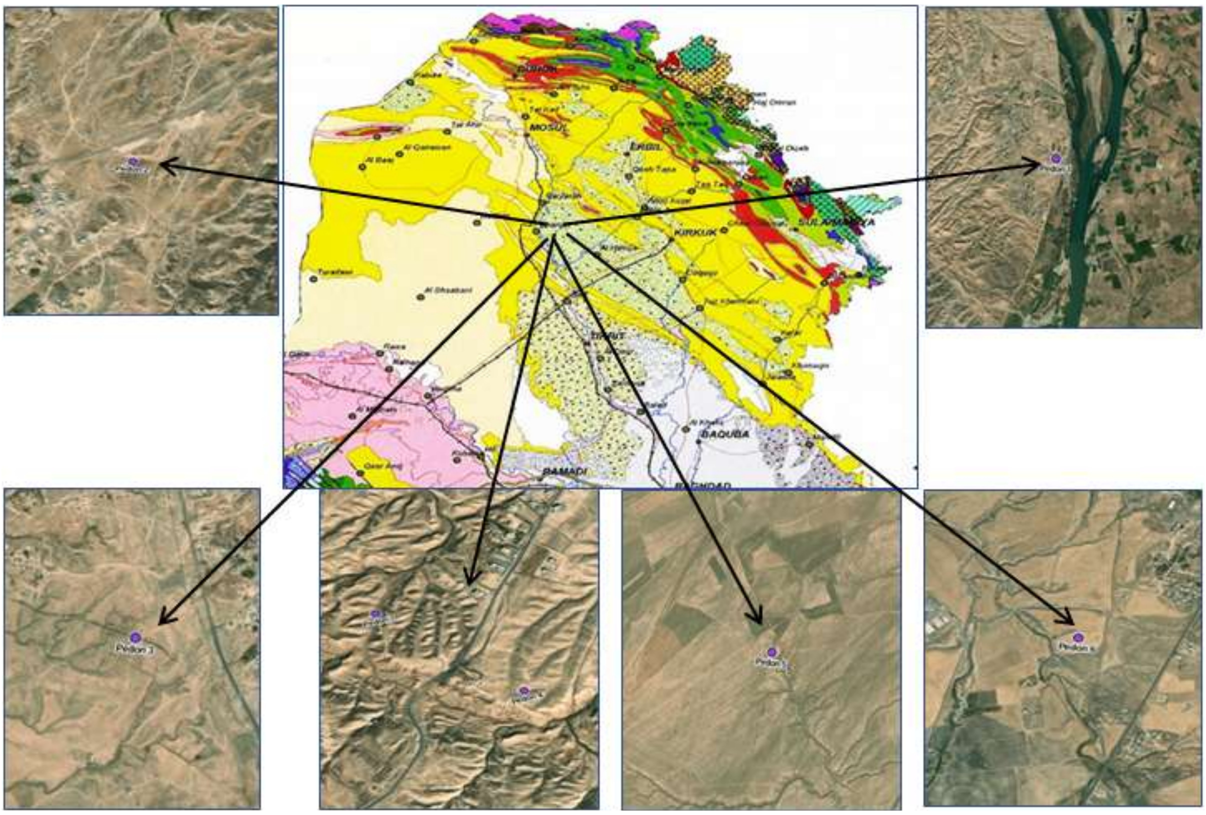

Figure 1. Map showing study locations
.

Table 1. The coordinates of the study areas

Longitude (DMS)	Latitude (DMS)	Location
43° 15′ 59.64″ E	35° 26′ 28.24″ N	P_1
43° 14′ 24.55″ E	35° 25′ 32.89″ N	P_2
43° 13′ 48.92″ E	35° 25′ 14.09″ N	P_3
43° 14′ 37.00″ E	35° 26′ 16.69″ N	P_4
43° 14′ 19.34″ E	35° 22′ 18.53″ N	P_5
43° 12′ 26.79″ E	35° 25′ 59.33″ N	P_6
43° 14′ 20.11″ E	35° 26′ 30.92″ N	P_7

and electrical conductivity (EC) were measured in a 1:2.5 soil–water suspension **[27]**. Organic matter was determined using the Walkley–Black wet oxidation method **[28]**. Calcium carbonate was determined by titration **[29]**, and gypsum content was estimated using the acetone precipitation method **[27]**. Thin Section Preparation, The micromorphological properties were studied using the thin section method. Undisturbed soil samples were selected in the same orientations across horizons, following the method of **[30]** and **[31]**.

Araldite gum and hardener were used in ratios ranging from 1:3 to 1:4.

2.5 XRF analysis

Elemental analysis of the oxides in the study samples was performed using X-ray fluorescence spectroscopy (XRF). The analysis focused on Fe_2O_3, SiO_2, Na_2O, K_2O, CaO, MgO, MnO, and TiO_2 in the sand particles Table 2. A separate portion of the soil samples was then collected, and 4 grams of this ground sample were mixed with wax to prepare compressed granules in the form of discs. These discs were subsequently placed in a Spectro XLAB 2000 X-ray fluorescence spectrometer for analysis. The analysis was performed in the laboratory of Soran University/Erbil.

2.6 Thin section

preparation Thin sections, 30 microns thick, were prepared from undisturbed soil samples to study pedogenic features using a transmitted polarized light microscope (German Leitz model) with 40x magnification. Pedogenic phenomena, such as coatings, crystals, and aggregates, were examined following the methods outlined by studies **[32] [33]**.

Table 2. Weathering Indicators used in the analysis

Weathering evidence	Definition	The equation	Source
(CIA)	Chemical Index of Alteration	Al2O3/(Al2O3+CaO+K2O+Na2O) ×100	[34]
(CIW)	Chemical Index of Weathering	Al2O3/(Al2O3+CaO+Na2O) ×100	[35]
(WIP)	Weathering Index of Parker	(2K2O/0.25) + (2Na2O/0.35) + (CaO*/0.7) +(MgO/0.9) ×100	[36]
(VR)	Vogt's Ratio	(Al2O3+K2O) /(MgO+CaO+Na2O)	[37]
(PWI)	Product of Weathering Index	[SiO2/ (TiO2+Fe2O3+SiO2+Al2O3)] × 100	[38]
(PIA)	Plagioclase Index of Alteration	(Al2O3-K2O)/ (Al2O3+CaO*+ Na2O-K2O) × 100	[39]
(ICV)	Index of compositional variability	[(Fe2O3+K2O+Na2O+CaO+MgO+MnO+ TiO2)] / (Al2O3)	[40]
WR	Weathering Ratio	(Na2O +CaO +MgO)/(TiO2)	[41]
WI	Weathering Index	(SiO2+ CaO) / (Fe2O3+Al2O3+ TiO2)	[42]

RESULT AND DISCUSSION

3.1 Soil physical and Chemical properties

It was observed that some horizons classified as clay-textured (C) in the studied sections, particularly in P_5 and P_6, contained very high clay content, reaching up to 430g.kg^{-1}, reflecting a clear development in the subsurface horizon due to clay depositional processes Table3 . The results also showed significant variation in the proportions of sand, silt, and clay among the different Pedons, with sand ranging from 190 - 642.5 g.kg^{-1}, silt from 177.5 - 640 g.kg^{-1}, and clay from 60 - 430 g.kg^{-1}. This indicates that soil properties vary depending on the parent material and pedogenic conditions across the sites. It was also shown that there is a clear effect of depth in some Pedons, where the soil texture changes from loamy or silty loamy textures in the surface horizons to finer textures (clayey or silty clayey) in the subsurface horizons, as in P_5 and P_6, which reflects the redistribution of fine particles within the section.

The results showed that the soil pH ranged from 6.70 - 8.31, indicating that the

ISSN 2072-3857

studied soils range from neutral to slightly alkaline, a common characteristic of soils in arid and semi-arid regions. Electrical conductivity (EC) ranged from 1.64 - 24.50 $dS.m^{-1}$, indicating a clear variation in salinity between horizons, with some samples recording high values reflecting salt accumulation conditions. Organic matter content ranged from 1.38 - 41.40 $g.kg^{-1}$, with a relative decrease observed in most subsurface horizons compared to the surface. The results also showed a significant increase in gypsum content, ranging from 0.72-847.84$g.kg^{-1}$, indicating the predominance of gypsum soils in several of the ponds. The calcium carbonate content ranged from 85 - 390 $g.kg^{-1}$, indicating the predominant calcareous nature of these soils. Overall, these results reflect the influence of arid climate in promoting the accumulation of salts, gypsum, and lime within the silt beds, with clear spatial and depth variations among the studied beds.

Table 3. Soil Physical and Chemical Properties

Pedon	Horizon	Depth	Sand	Silt	Clay	Texture	pH	EC	OM	Gypsum	$CaCO_3$
		cm	$g.kg^{-1}$	$g.kg^{-1}$	$g.kg^{-1}$			dSm^{-1}	$g.kg^{-1}$	$g.kg^{-1}$	$g.kg^{-1}$
P_1	A	0-30	555	215	230	SCL	8.31	2.81	41.40	3.57	200
	B_{y1}	30-60	555	365	80	SL	6.88	4.19	2.76	197.98	290
	B_{y2}	60-99	287.5	627.5	85	SiL	7.83	4.01	4.14	244.87	290
	C_k	99-111+	605	202.5	192.5	SL	7.65	5.10	2.76	7.15	315
P_2	A	0-21	300	365	335	CL	8.15	1.87	12.42	0.72	290
	B_k	21-48	627.5	217.5	155	SL	7.96	3.15	9.66	24.06	315
	C_{ky1}	48-110	275	640	85	SiL	6.74	2.74	1.38	423.42	225
	C_{ky2}	110-143+	475	440	85	L	7.15	2.95	2.76	327.19	175
P_3	A	0-30	642.5	177.5	180	SL	7.63	1.64	8.28	5.74	300
	B_{tk}	30-50	315	430	255	L	7.48	2.87	4.14	8.66	390
	C_{y1}	50-118	450	490	60	SL	7.50	3.25	4.14	789.62	135
	C_{y2}	118-160+	537.5	377.5	85	SL	7.44	2.92	2.76	592.57	125
P_4	A	0-7	525	390	85	SL	7.80	2.79	6.90	749.00	150
	C_{y1}	7-29	475	440	85	L	7.61	2.44	4.14	668.41	140
	C_{y2}	29-60+	387.5	515	97.5	SiL	7.51	4.76	2.76	847.84	85
P_5	A	0-13	240	505	255	SiL	7.86	3.08	20.70	1.42	245

ISSN 2072-3857

	B_t	13-47	215	370	415	C	8.11	3.22	12.42	9.99	270
	C_{ky1}	47-68	325	590	85	SiL	7.43	2.79	9.66	333.95	275
	C_{ky2}	68-92	425	502.5	72.5	SiL	6.99	3.24	2.76	526.57	275
	C_{ky3}	92-115+	312.5	627.5	60	SiL	6.70	2.56	2.76	632.86	180
P_6	A	0-20	277.5	530	192.5	SiL	7.63	2.87	13.80	17.05	210
	B_{tk}	20-63	190	380	430	C	6.99	3.31	9.66	2.84	345
	C_{ky1}	63-107	400	515	85	SiL	6.97	3.50	6.90	453.68	190
	C_{ky2}	107-150+	400	540	60	SiL	7.33	3.48	4.14	535.68	225
P_7	A	0-23	265	580	155	SiL	7.04	16.98	9.66	23.65	255
	C_k	23-37	415	455	130	L	7.43	9.72	6.90	49.67	260
	C_{kyz1}	37-64	365	505	130	SiL	6.92	24.50	9.66	167.28	255
	C_{kyz2}	64-111+	412.5	490	97.5	L	7.00	13.46	6.90	257.71	265

3.2 Weathering Indicators analysis

The data presented in Table 4 indicate substantial variability in the major oxide composition among the studied pedons and their genetic horizons, reflecting differences in parent material, pedogenic processes, and secondary accumulation under arid to semi-arid environmental conditions. Silicon dioxide SiO_2 was the dominant oxide in most surface and subsurface horizons, reaching its highest value of 49.41% in P5 horizon A, followed closely by 48.22% in P_1 horizon A, whereas the lowest value 9.60% occurred in P_4 horizon C_{y1}. The higher SiO_2 contents in upper horizons suggest the relative abundance of quartz and other resistant silicate minerals, while the lower values in some subsurface horizons may be attributed to dilution by gypsum and carbonate accumulations.

Calcium oxide CaO showed marked variation, ranging from 17.21% in P_5 horizon A to 39.90% in P_4 horizon A, indicating strong calcareous influence and widespread carbonate enrichment in several pedons. Elevated CaO concentrations are typical of soils formed in dry regions where carbonate dissolution is limited and upward movement of calcium-bearing solutions promotes secondary calcification. Sulfur trioxide SO_3 exhibited the greatest variability, with a minimum value of 0.787% in P_6 horizon Btk and a maximum of 43.15% in P_4 horizon C_{y1}, confirming intense gypsum accumulation in selected horizons, especially within C_y and C_{ky} horizons. This pattern reflects evaporative concentration and translocation of sulfate minerals in moisture-deficient settings.

Aluminum oxide Al_2O_3 values ranged from 3.24% in P_4 horizon A to 14.15% in P_5 horizon B_t, while iron oxide Fe_2O_3 ranged between 1.16% in P_4 horizon C_{y1} and 7.40% in P_1 horizon A. Higher Al_2O_3 and Fe_2O_3 values in B_t and B horizons may indicate finer-textured materials, clay illuviation, and relative concentration of sesquioxides following

ISSN 2072-3857

weathering losses of more mobile constituents. Magnesium oxide MgO ranged from 1.89% - 9.05%, suggesting contributions from dolomitic or ferromagnesian minerals and partial association with carbonate phases.

Table 4. Percentage of major element oxides the studied Pedons using the XRF device

Pedons	Horizon	Depth	SiO_2 %	CaO %	SO_3 %	Al_2O_3%	MgO %	Fe_2O_3%	K_2O %	Na_2O%	TiO_2 %	MnO %
P_1	A	0-30	48.22	17.80	1.167	13.42	7.71	7.40	1.99	1.36	0.78	0.16
	B_{y1}	30-60	39.53	22.89	8.117	11.30	7.10	6.99	1.76	1.56	0.64	0.124
	B_{y2}	60-99	37.72	24.50	9.621	11.07	6.92	5.75	1.64	1.70	0.98	0.108
	C_k	99-111+	-	-	-	-	-	-	-	-	-	-
	Average		41.82	21.73	6.30	11.93	7.24	6.71	1.80	1.54	0.80	0.13
P_2	A	0-21	47.16	17.80	1.047	13.85	9.01	7.07	2.08	1.24	0.64	0.093
	B_k	21-48	45.01	19.78	6.118	12.28	7.54	6.35	1.71	0.44	0.69	0.084
	C_{ky1}	48-110	27.76	26.00	25.32	8.44	6.75	3.83	1.10	0.41	0.33	0.05
	C_{ky2}	110-143+	-	-	-	-	-	-	-	-	-	-
	Average		39.98	21.19	10.83	11.52	7.77	5.75	1.63	0.69	0.55	0.08
P_3	A	0-30	47.58	22.37	1.05	12.94	6.05	6.34	1.70	1.25	0.68	0.05
	B_{tk}	30-50	22.13	33.83	30.01	6.63	3.60	3.02	0.46	0.21	0.13	0.00
	C_{y1}	50-118	15.58	32.73	39.31	5.19	3.61	2.54	0.53	0.21	0.23	0.053
	C_{y2}	118-160+	-	-	-	-	-	-	-	-	-	-
	Average		28.43	29.64	23.46	8.25	4.42	3.97	0.90	0.56	0.35	0.03
P_4	A	0-7	12.05	39.90	39.58	3.24	1.89	2.44	0.40	0.09	0.35	0.05
	C_{y1}	7-29	9.60	39.32	43.15	3.28	2.32	1.16	0.37	0.69	0.10	0.022
	C_{y2}	29-60+	18.82	35.08	32.13	5.54	3.62	2.42	0.90	1.22	0.28	0.00
	Average		13.49	38.10	38.29	4.02	2.61	2.01	0.56	0.66	0.24	0.02

P_5	A	0-13	49.41	17.21	1.275	13.69	7.01	6.98	2.10	1.28	0.88	0.168
	B_t	13-47	46.61	20.14	0.909	14.15	7.21	6.78	2.15	1.21	0.70	0.147
	C_{ky1}	47-68	39.44	20.51	10.19	11.99	8.39	6.52	1.27	0.94	0.60	0.139
	C_{ky2}	68-92	-	-	-	-	-	-	-	-	-	-
	C_{ky3}	92-115+	32.60	22.07	19.29	9.86	9.05	4.33	1.24	1.02	0.49	0.053
	Average		42.02	19.98	7.91	12.42	7.92	6.15	1.69	1.11	0.67	0.13
P_6	A	0-20	46.82	18.51	5.681	12.94	6.54	5.89	1.77	1.17	0.61	0.079
	B_{tk}	20-63	43.66	25.87	0.787	13.13	6.75	6.19	1.70	1.19	0.66	0.058
	C_{ky1}	63-107	23.45	30.49	28.48	7.30	4.40	3.47	0.93	1.04	0.37	0.069
	C_{ky2}	107-150+	-	-	-	-	-	-	-	-	-	-
	Average		37.98	24.96	11.65	11.12	5.90	5.18	1.47	1.13	0.55	0.07
P_7	A	0-23	42.83	19.57	7.625	11.50	6.65	7.30	1.81	2.65	0.06	0.00
	C_k	23-37	42.00	20.70	5.202	12.21	7.89	6.23	2.23	2.84	0.60	0.081
	C_{kyz1}	37-64	-	-	-	-	-	-	-	-	-	-
	C_{kyz2}	64-111+	32.22	23.55	18.36	8.90	6.35	5.44	1.56	2.94	0.58	0.091
	Average		39.02	21.27	10.40	10.87	6.97	6.32	1.87	2.81	0.42	0.06

Potassium oxide K_2O and sodium oxide Na_2O generally occurred in lower concentrations, where K_2O varied from 0.37% - 2.23%, and Na_2O from 0.09% to 2.94%. Their distribution likely reflects differences in feldspar abundance, clay mineral weathering, and localized salinity effects. Titanium oxide TiO_2, commonly regarded as a relatively immobile oxide, ranged from 0.06% in P_7 horizon A to 0.98% in P_1 horizon B_{y2}. The very low TiO_2 content in some horizons contributed to exceptionally high weathering ratio values, particularly in P_7, where the C_k horizon recorded a value of 458.77, due to the extremely low concentration of resistant titanium-bearing minerals.

Overall, the geochemical composition of these pedons reveals the combined effects of lithological discontinuity, carbonate and gypsum accumulation, clay translocation, and differential weathering intensity. The enrichment of CaO and SO_3 in subsurface horizons, coupled with declining SiO_2 in some profiles, supports the predominance

ISSN 2072-3857

of calcification and gypsification as major pedogenic pathways in the study area.

The results presented in Table 5 demonstrate clear variability in the weathering Indicators among the studied pedons and their diagnostic horizons, reflecting differences in parent material composition, pedogenic evolution, and the influence of carbonate and gypsum accumulations under arid to semi-arid environmental conditions.

The Chemical Index of Alteration CIA values ranged from 7.43% in the surface horizon of P_4 to 39.93% in the surface horizon of P_5, with mean values varying between 9.30% in P_4 and 35.23% in P_5. Similarly, the Chemical Index of Weathering CIW ranged from 7.50% in P_4 to 42.54% in P_5, with mean values between 9.44% and 37.05%, respectively. These generally low values indicate weak hydrolytic weathering and limited removal of mobile base cations (Ca, Na, K), suggesting that feldspar alteration was minor in most pedons. The relatively higher values in P5 and P1 indicate slightly more advanced chemical alteration, possibly associated with better drainage conditions or longer pedogenic stability.

The Plagioclase Index of Alteration PIA values followed a similar trend, ranging from 6.62% in P_4 to 38.53% in P_5, with average values between 8.25% and 33.76%. This confirms that plagioclase weathering was generally weak throughout the study area, particularly in P_4 where high carbonate and gypsum contents suppressed silicate alteration processes. The higher PIA values in P_5 may indicate comparatively greater decomposition of plagioclase minerals and partial clay neoformation.

In contrast, the Parker Weathering Index WIP showed relatively high values in all pedons, ranging from 5281.72 - 7246.72, with average values between 5592.96 in P2 and 6913.37 in P_7. Such high WIP values indicate that substantial amounts of mobile alkali and alkaline earth elements are still retained within the soil matrix, reflecting weak leaching intensity and relatively fresh parent materials. The exceptionally high values in P_7, particularly in the C_k horizon7246.72, suggest strong enrichment of exchangeable and carbonate-associated bases.

The Vogt Ratio VR ranged from 0.09 in P_4 to 0.62 in P_5, with mean values between 0.11 and 0.49. Low VR values indicate the predominance of aluminum-poor, base-rich materials, especially in calcareous and gypsiferous pedons such as P_4. Conversely, the higher values in P_5 suggest a relatively greater proportion of aluminosilicate minerals and moderate silicate weathering compared with other pedons.

The Product Index PWI values were relatively consistent, ranging from 66.16 - 70.66%, indicating only modest differences in mineralogical maturity among pedons. Slightly lower values in some gypsiferous horizons may reflect dilution by secondary evaporite minerals rather than advanced weathering.

The Index of Compositional Variability ICV displayed marked differences, ranging from 2.60 in P_5 horizon A to 13.92 in P_4 horizon A. Mean values varied from 3.10 in P_5 to 11.73 in P_4. High ICV values, especially in P_4 and some horizons of P_3, indicate the dominance of unstable primary minerals and limited transformation into secondary clay minerals, reflecting immature soil development and weak pedogenesis. In contrast, lower ICV values in P_5 suggest comparatively greater mineral alteration and clay enrichment.

The Weathering Index WI values ranged from 3.01 in P_2 horizon A to 10.79 in P_4 horizon C_{y1}. Higher WI values in P_4 and P_3 horizons indicate the strong influence of gypsum and carbonate accumulation, which modified the geochemical balance of resistant and mobile oxides. Lower WI values in P_1, P_5, P_7 indicate comparatively less geochemical disturbance.

The Weathering Ratio WR showed the widest variability, ranging from 28.91 in P_5

ISSN 2072-3857

horizon A to 458.77 in P_7 horizon A, with mean values between 39.36 in P1 and 229.41 in P_4. Exceptionally high WR values were also observed in P_4 horizon C_{y1} 426.07 and P_3 horizon B_{tk} 293.15. These elevated values are mainly attributed to the very low concentrations of TiO_2 , a resistant oxide commonly used in denominator-based weathering ratios. In P_7 horizon A, TiO_2 reached only 0.06%, causing a sharp increase in WR. Likewise, low TiO_2 contents in gypsiferous horizons of P_4 contributed to the high WR values there. This demonstrates that WR is highly sensitive to resistant element depletion or dilution by carbonate and sulfate minerals.

Overall, the collective behavior of all Indicators confirms that the studied soils are characterized by weak chemical weathering, dominance of physical weathering, limited silicate mineral transformation, and immature pedogenic development. The accumulation of carbonates and gypsum significantly lowered CIA, CIW, and PIA values while increasing WIP, WI, and WR values. These trends are fully consistent with soils developed under arid to semi-arid climatic conditions, where low rainfall, restricted leaching, and strong evaporation promote calcification and gypsification rather than intensive chemical weathering.

Table.5 Weathering index values for the study area

Pedons	Horizon	Depth	CIA	CIW	WIP	VR	PWI	PIA	ICV	WI	WR
P_1	A	0-30	38.83	41.19	5763.79	0.57	69.07	37.38	2.77	3.06	34.61
	B_{y1}	30-60	30.12	31.60	6356.59	0.41	67.63	28.06	3.63	3.30	49.66
	B_{y2}	60-99	28.45	29.70	6550.99	0.38	67.94	26.46	3.76	3.50	33.81
	C_k	99-111+									
	Average		32.47	34.17	6223.79	0.46	68.21	30.63	3.39	3.28	39.36
P_2	A	0-21	39.60	42.11	5918.10	0.57	68.62	38.19	2.74	3.01	43.63
	B_k	21-48	35.91	37.80	5281.72	0.50	69.97	34.34	2.98	3.35	40.34
	C_{ky1}	48-110	23.49	24.23	5579.07	0.29	68.76	21.75	4.56	4.26	99.56
	C_{ky2}	110-143+									
	Average		33.00	34.71	5592.96	0.45	69.12	31.43	3.43	3.54	61.18
P_3	A	0-30	33.83	35.40	5938.90	0.49	70.45	32.25	2.97	3.51	43.86
	B_{tk}	30-50	16.11	16.29	5717.28	0.19	69.37	15.35	6.22	5.73	293.15
	C_{y1}	50-118	13.43	13.62	5623.52	0.16	66.16	12.39	7.69	6.06	156.08
	C_{y2}	118-160+									
	Average		21.12	21.77	5759.90	0.28	68.66	20.00	5.63	5.10	164.36

ISSN 2072-3857

P_4	A	0-7	7.43	7.50	6282.82	0.09	66.64	6.62	13.92	8.61	120.13
	C_{y1}	7-29	7.51	7.57	6561.88	0.09	67.92	6.78	13.41	10.79	426.07
	C_{y2}	29-60+	12.96	13.24	6829.26	0.16	69.54	11.34	7.86	6.54	142.04
	Average		9.30	9.44	6557.99	0.11	68.03	8.25	11.73	8.65	229.41
P_5	A	0-13	39.93	42.54	5648.99	0.62	69.64	38.53	2.60	3.09	28.91
	B_t	13-47	37.60	39.87	6087.65	0.57	68.31	35.99	2.71	3.09	40.89
	C_{ky1}	47-68	34.55	35.86	5418.14	0.44	67.36	33.33	3.20	3.14	49.91
	C_{ky2}	68-92									
	C_{ky3}	92-115+	28.84	29.93	5732.34	0.35	68.96	27.18	3.88	3.72	65.70
	Average		35.23	37.05	5721.78	0.49	68.56	33.76	3.10	3.26	46.35
P_6	A	0-20	37.63	39.67	5451.41	0.56	70.66	36.21	2.67	3.36	42.77
	B_{tk}	20-63	31.35	32.68	6485.80	0.44	68.60	29.70	3.23	3.48	51.10
	C_{ky1}	63-107	18.36	18.80	6183.31	0.23	67.79	16.81	5.59	4.84	96.73
	C_{ky2}	107-150+									
	Average		29.11	30.38	6040.17	0.41	69.02	27.57	3.83	3.89	63.53
P_7	A	0-23	32.37	34.11	6499.04	0.46	69.43	30.36	3.31	3.31	458.77
	C_k	23-37	32.14	34.15	7246.72	0.46	68.80	29.76	3.32	3.29	51.99
	C_{kyz1}	37-64									
	C_{kyz2}	64-111+	24.10	25.16	6994.35	0.32	68.33	21.72	4.55	3.73	56.19
	Average		29.54	31.14	6913.37	0.41	68.85	27.28	3.73	3.45	188.98

3.3 Thin section preparation

3-3-1- Thin Section (P_1-B_{y1})

The results of microscopic examinations of thin sections of undisturbed soil samples from the B_{y1} subsurface horizon of the first pedun in the Al-Hasuwaya area showed a predominance of a complex structure consisting of a subangular blocky structure and a spongy structure. The results also showed different sizes and shapes of gypsum crystals, including lenticular, spindle, and granular shapes, as well as the presence of incompletely oriented gypsum crystals due to dissolution processes. This indicates a complete filling of coarse, semi-rhomboidal (C-Gy) gypsum crystals surrounded by soil material (SL) and gypsum grain clusters, held together by a calcite matrix (Cal). The presence of lime in these forms is directly related to the transported calcareous formations that are abundant in Iraqi soils, and to the residual or transported parent material. Transported, with an abundance and diversity of interstitial pore shapes in this horizon (Po) resulting from the dissolution of gypsum particles. **[30]** demonstrated that the size, shape, and arrangement of interstitial pores play a significant role in the movement and transport of water from one place to another within the soil body, and thus contribute to soil formation Figure 2.

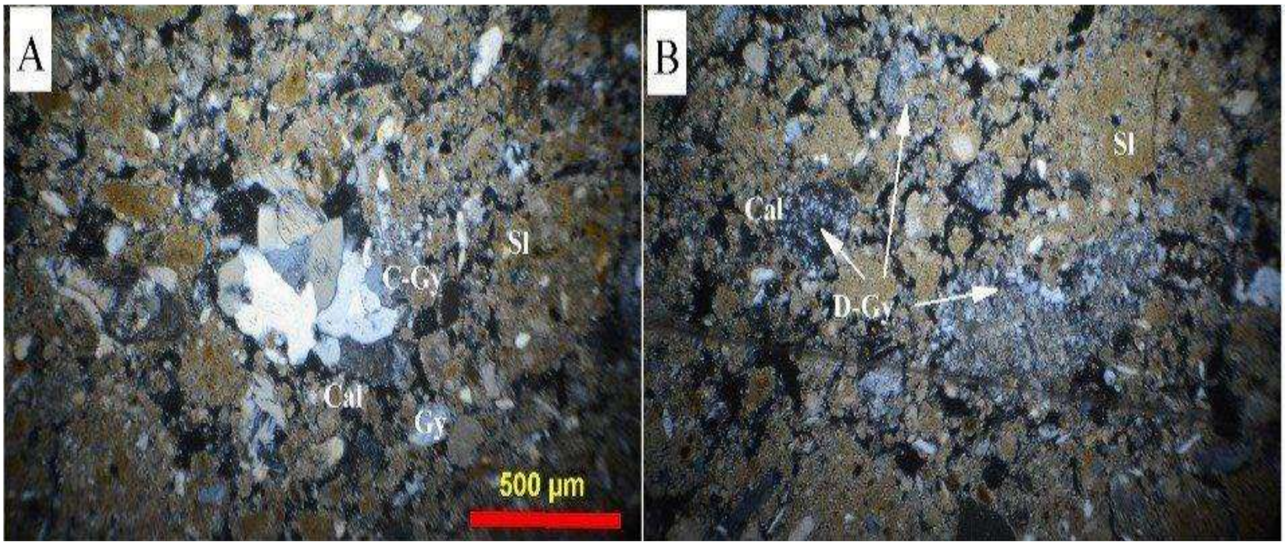

Figure 2. B_{y1} horizon for the P_1

3-3-2- Thin Section (P_2-C_{ky1})

The subsurface horizon Cky1 of the second pedun in the Tel Ismail area shows that the sub-angular blocky structure has varying sizes, and the presence of granular structure appears in different types of slabs, making many pores and voids in small shapes in most of the views under the microscope (packing voids). Large, unconnected compound packing voids and chamber voids appear as circular vesicles between small and medium. Some gypsum and carbonate structures have been transferred to them and settled in the inner edges of the voids. There is also the presence of secondary calcite deposits in the form of slanted needles in the voids of the pore walls (infilling micritic pedogenic carbonate), which may originate from surface additions by wind or water erosion. The results also showed the presence of a porphyroblastic texture of nodular gypsum, with fine-grained and spindle-shaped gypsum of varying sizes and types, surrounded by fine-grained soil material. Furthermore, nodules were present, distributed throughout the layer. There were carbonate nodules, as well as some reddish-yellow quartz nodules. The overlap and co-occurrence of different types of cutans confirms that this soil underwent different formation conditions Figure 3.

ISSN 2072-3857

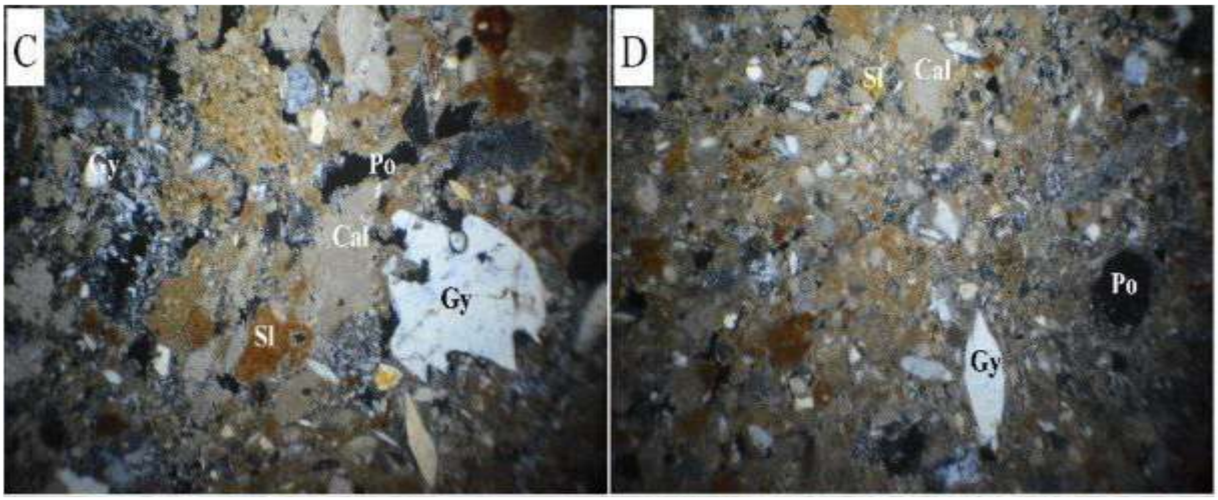

The structure in this panel is of the Complex microstructure type, which is composed of a mixture of two or more types. Specifically, it consists of a subangular blocky structure and a granular structure in the thin section of the soil. The variation in the type and degree of clarity of the structure from one view to another of the same panel corresponds to the variation in the type and quantity of components in this horizon, which in turn affects the degree of bonding between these components. Complex filling is observed between coarse rock fragments, minerals, and soil aggregates of varying sizes. There are also discontinuous voids with irregular shapes and walls, called vughs. The presence of gypsum in this panel is noted, exhibiting typical first-order gray and white interlacing colors. The crystals exhibit lenticular to needle-like shapes throughout the panel, along with the presence of irregularly oriented gypsum crystals resulting from dissolution processes. These crystals vary in size, ranging from small, silt-like particles to large, coarse or very coarse sand-like particles, depending on the soil's evolutionary state. This variation is reflected in the growth of the gypsum aggregates over time. The results also indicate the presence of soluans on the outer surfaces of the intercalary spaces, composed of crystalline salts. Additionally, there are white nodules of calcium carbonate in the form of small, irregularly shaped aggregates resulting from pedigenous processes Figure 4.

Figure 4. C_{y1} horizon for the P_3

3-3-4- Thin Section (P_4-C_{y2})

The structure in this slab is of the subangular blocky microstructure type. Short, flat voids separate the angular blocks on all or most sides. Other voids, such as small channels or cavities, may also be present within or between the aggregates. Finally, the surfaces of the aggregates fit together well. Complex packing is observed between coarse rock fragments, minerals, and soil aggregates of varying sizes. There are also discontinuous voids with irregular shapes and walls, called vughs. Furthermore, there is an abundance and variety of interstitial pore shapes in this slab, which are of the simple packing void type. This is due to the random arrangement and compression of

ISSN 2072-3857

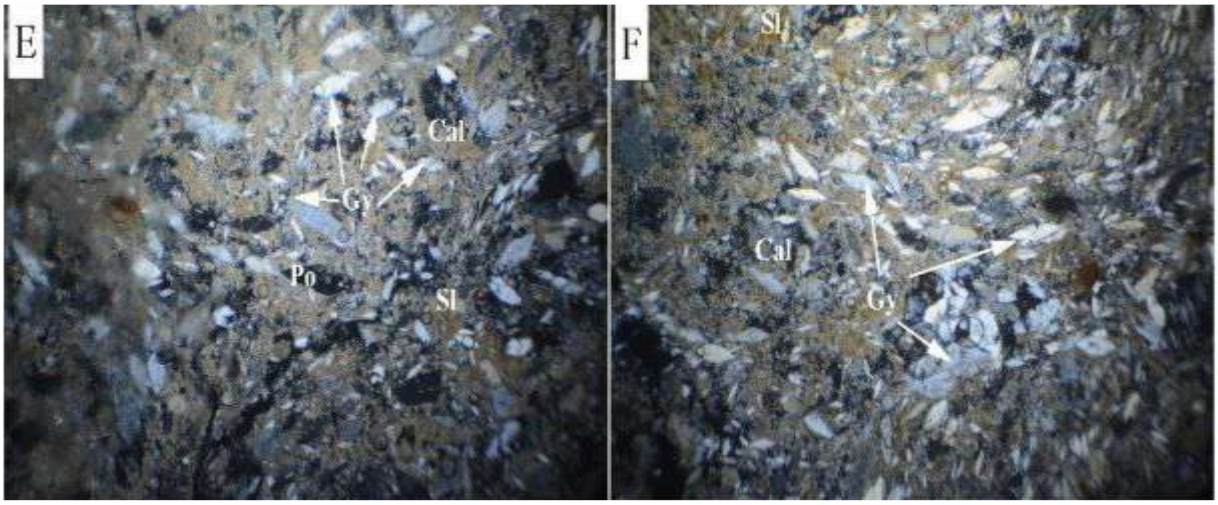

primary grains. The slide shows a complete filling of coarse-grained, semi-the entire slide. The upper portion exhibits a sugary (granular) form filling the pores, surrounded by soil material (Sl) and clusters of gypsum grains bound to a calcite matrix (Cal). This matrix exhibits high porosity (Po) due to the dissolution of the gypsum grains. No coating activity was observed, and relatively small white and reddish-yellow nodules were distinguishable across the same area Figure 5.

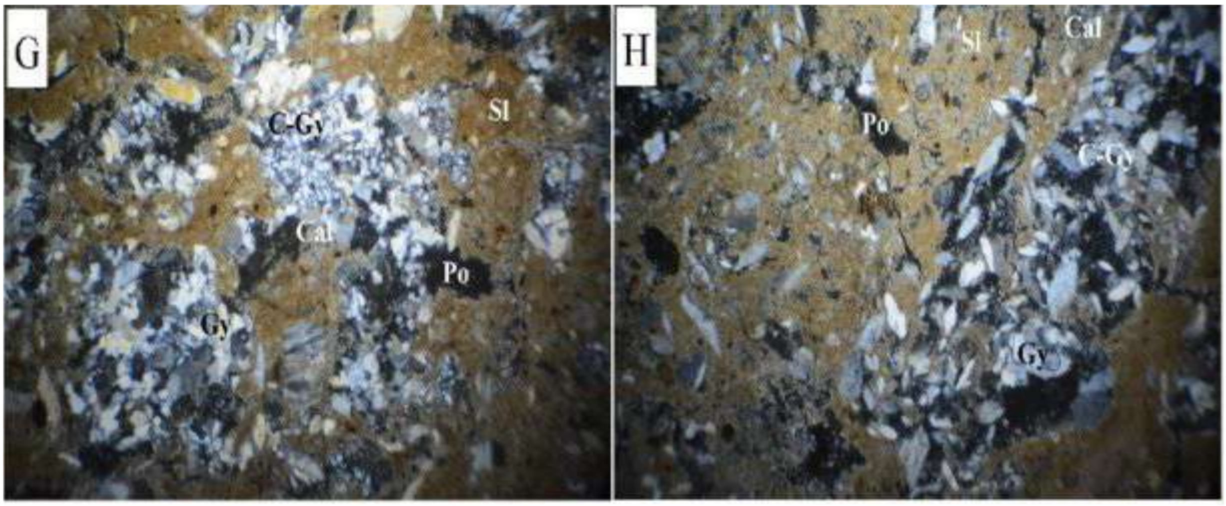

Figure 5. C_{y2} horizon for the P_4

3-3-5- Thin Section (P_5-C_{ky2})

The panel shows a subangular blocky microstructure and a sparse granular structure. The voids were filled with a composite filling of unconsolidated grains forming subangular blocks of varying sizes and shapes. Some voids were irregular, depending on the surrounding grains, while others were channel-shaped voids, possibly due to the presence of microorganisms. Film formation was very rare. Nodules of varying sizes were observed, appearing as white globules. Additionally, there was discontinuous filling of gypsum grains (D-Gy) surrounded by fine-grained soil material (Sl) and small amounts of gypsum

ISSN 2072-3857

grains (Gy), along with calcite masses and clusters (Cal), and a high degree of gypsum solubility (Po) Figure 6.

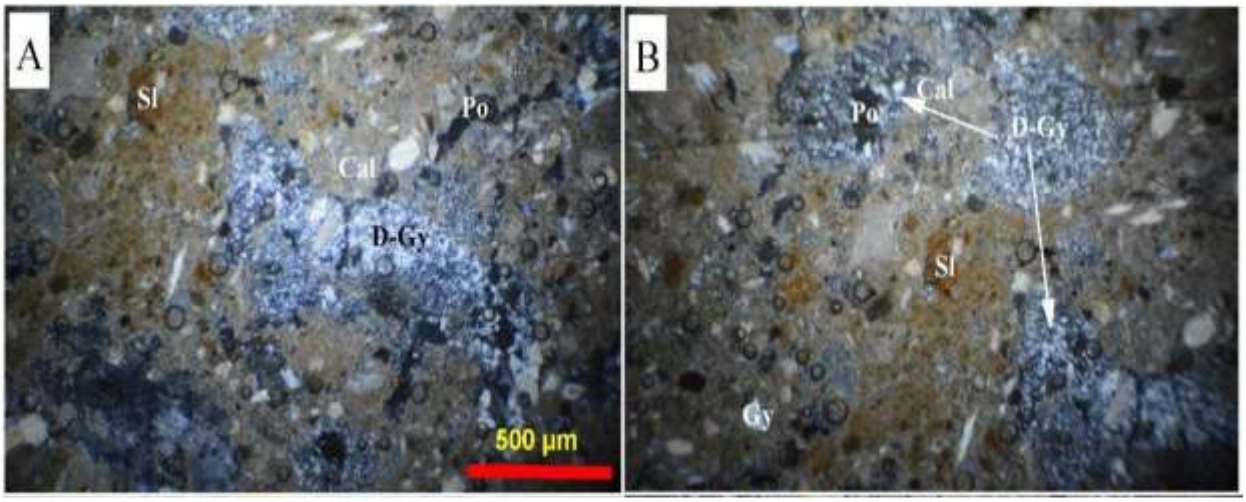

some parts of the slice and angular-block for most of the slice with non-rounded edges and irregular geometric shapes. Large, unconnected Compoundpacking voids and Chambers voids appeared, which appear as circular vesicles between small and medium-sized ones. Some gypsum and carbonate structures were transferred to them and settled in the inner edges of the voids. The results also showed complete material (Sl) and clusters of gypsum grains, linked by a matrix of calcite (Cal), with an increase in porosity (Po) as a result of gypsum dissolution. In addition, structures made up of clusters of fine soil material (Sl) surrounded by occurrences of lenticular gypsum (Gy), with a ground mass of calcite (Cal), and pores resulting from gypsum dissolution (Po) Figure 7.

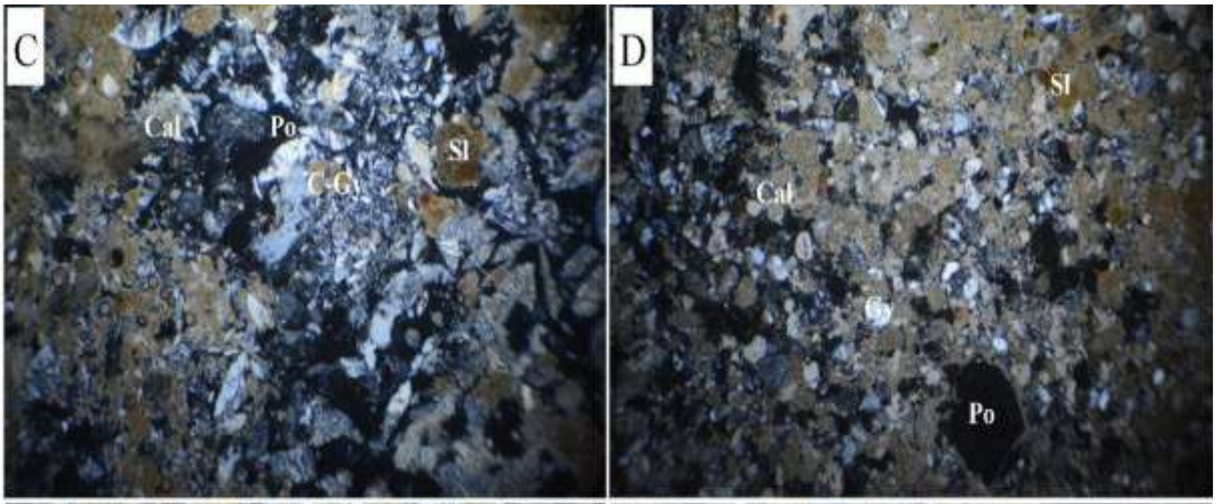

Figure 7. C_{ky1} horizon for the P_6

3-3-7- Thin Section (P_7-C_{kyz2})

The panel ( ) showed that the soil structure was of the complex microstructure type, which is a complex structure composed of a mixture of two or more types, consisting of a sub-angular blocky structure, an angular blocky structure, and a granular structure in the thin section. The voids were filled with a composite filling between unconsolidated particles into sub-

ISSN 2072-3857

angular blocks of varying sizes and shapes, some irregular (vugs) depending on the surrounding particles, and others in the form of channels (voids). In addition, the presence of vesicles, which are round spaces often observed in groups, usually indicates the presence of air bubbles in the soil. The panel reveals a composition of fine-grained soil (Sl) aggregates surrounded by lenticular gypsum (Gy) deposits. Plagioclase feldspar grains in the thin sections are identified by the characteristic albite twinning pattern, appearing as parallel bands with alternating quenching, indicating an igneous origin of the parent material and a low to moderate degree of weathering. Calcite (Cal) aggregates and porosity resulting from the dissolution of gypsum grains (Po) are also present Figure 8.

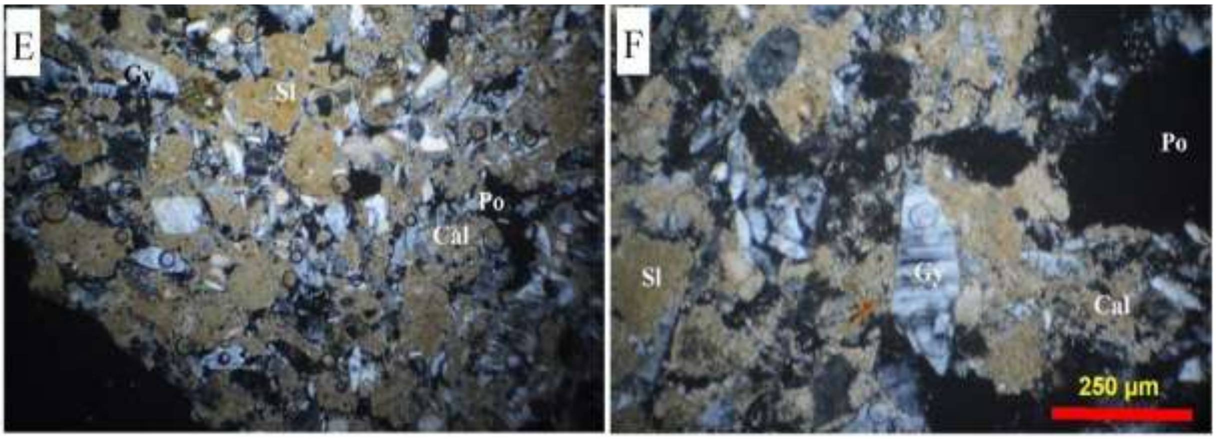

Figure 8. C_{kyz2} horizon for the P_7

Conclusion

The results indicate that the soils of Al-Shirqat district are characterized by the dominance of gypsophilic and calcareous processes and the accumulation of salts within the soil profile due to limited leaching in the arid to semi-arid climate. Chemical weathering is less intense than physical weathering, resulting in the soil retaining a high percentage of primary minerals and exhibiting moderate to weak pedogenic development. The variation among the seven Pedons is linked to differences in the parent material and local geomorphological conditions. Microscopic and geochemical evidence confirms successive cycles of dissolution and re-deposition of gypsum and carbonates, representing the distinctive geological and pedogenic characteristics of the region's soils.

Acknowledgments

The authors would like to express their sincere gratitude to all individuals and institutions who contributed to the completion of this research. Special thanks are extended to the academic staff and colleagues for their valuable guidance, support, and constructive suggestions throughout the study.

Conflict of Interest

The authors declare that there is no conflict of interest regarding the publication of this paper.

Funding Declaration

This research received no specific grant from any funding agency in the public, commercial, or not-for-profit sectors.

Author Contributions

The first and second authors contributed to writing the original draft of the manuscript, as well as reviewing and editing the final version. Both authors have read and approved the final manuscript and agreed to its submission.

References

[1]Nicosia, C., & Stoops, G. (Eds.). (2017). Archaeological soil and sediment micromorphology. John Wiley&Sons.

[2]Sadiq, A. A. (2020). AN OVERVIEW OF SOIL MICROMORPHOLOGY

ISSN 2072-3857

TREND IN THE FIELD OF SOIL SCIENCE. African Jornal of Agriculture and Food Science, 3(2), 11-31.

[3]Cao, T., Wang, J.,&Zhang, H. (2022). The Significance of Soil Micromorphology Research in Land Reclamation. In E3S Web of Conferences (Vol. 338, p. 01042). EDP Sciences.

[4]Etedali, S., Abtahi, S. A., Salehi, M. H., Givi, J., Farpoor, M. H.,&Baghernejad, M. (2018). Chemical, physical, mineralogical and micromorphological properties of soils along a toposequence in Chelgerd region, Chaharmahal-va-Bakhtiari, Iran.

[5]Chakherloo, S. (2014). The study of genesis and micromorphological properties of saline–sodic soils of the west of Urmia Lake. Journal of Soil Management and Sustainable Production, 4(3), 87-111.

[6]Moazallahi, M.,&Farpoor, M. H. (2009). Soil micromorphology and genesis along a climotoposequence in Kerman Province, Central Iran.

[7]Neyestani, M.,&Farpoor, M. H. (2014). Genesis, clay mineralogy and micromorphology of saline-gypsiferous soils in Kheirabad playa, Sirjan. Journal of Arid Biome, 4(1), 65-78.

[8]Heeshan, A. M., Ismaeal, A. S.,&Rashid, A. A. (2022). Genesis and the degree of development of the clay and calcareous horizons of some soils in Northern Iraq. Int. J. Agricult. Stat. Sci. Vol, 18(1), 1617-1627. https://connectjournals.com /03899.2022.18.1617.

[9]Ismaeal, A. S. (2022). Diagnostics and Characterization of Micro morphological Features of some Soil Series in Baiji City, Central Iraq. Tikrit Journal for Agricultural Sciences, 22(2), 132-147.

[10]Mohammed, S. H.,&Wheib, K. A. (2024). Micromorphological characterization of salt affected soils of Alnajmi agricultural project in Muthanna governorate\southern of Iraq. Iraqi Journal of Agricultural Sciences, 55(6), 2074-2084.

[11]Wheib, K. A.,&Ibrahim, O. N. (2012). Study of morphological and micromorphological properties of some salt affected soils in the middle of Iraq. Iraqi J Agric. Sci, 43, 106-118.

[12]Wieder, M.,&Yaalon, D. H. (1982). Micromorphological fabrics and developmental stages of carbonate nodular forms related to soil characteristics. Geoderma, 28(3-4), 203-220.

[13]Yang, J., Que, S., Wang, T., Bi, Y., Li, N.,&Su, X. (2023). Diagnostic surface horizon vs. conventional surface horizon: The impact of topsoil delineation on the results of topsoil organic carbon density assessment in China. Catena, 229, 107198.

[14]Hashemi, S. S., M. Baghernejad and H. Khademi, 2011. Micro morphology of gypsum crystals in southern Iranian Soils under different moisture regimes,Agr. Sci. Tech. Vol. 13: 273- 288.

[15]Khormali, F. Abtahi, A., Mahmoodi, S. stoop. G.(2003). Argillic horizon development in calcareous soils of arid and semiarid regions of southern Iran . Catena 53. pp273-301.

[16]Hill, I. G., Worden, R. H.,&Meighan, I. G. (2000). Yttrium: the immobility-mobility transition during basaltic weathering. Geology, 28(10), 923-926.

[17]Eggleton, R. A., Foudoulis, C.,&Varkevisser, D. (1987). Weathering of basalt: changes in rock chemistry and mineralogy. Clays and Clay Minerals, 35(3), 161-169.

[18]Jin-long, M., Gang-Jian, W., Yi-Gang, X., WenGuo, L. and Wei-Dong, S., 2007. Mobilisation and redistribution of major and trace elements Special Papers-Geological Society of America, pp. 21-21. https://doi.org/10.1130/ SPE284-p21.

[19] Regassa, A., Van Daele, K., De Paepe, P., Dumon, M., Deckers, J., Asrat, A., & Van Ranst, E. (2014). Characterizing weathering intensity and trends of geological materials in the Gilgel Gibe catchment, southwestern Ethiopia.

Journal of African Earth Sciences, 99, 568-580.

[20] Arıkan, F., Ulusay, R., & Aydın, N. (2007). Characterization of weathered acidic volcanic rocks and a weathering classification based on a rating system. Bulletin of Engineering Geology and the Environment, 66(4), 415-430.

[21] Guan, P., Ng, C. W. W., Sun, M., & Tang, W. (2001). Weathering Indicators for rhyolitic tuff and granite in Hong Kong. Engineering Geology, 59(1-2), 147-159.

[22] Tunçay, T., & Dengiz, O. (2016). Chemical weathering rates and geochemical-mineralogical characteristics of soils developed on heterogeneous parent material and toposequence. Carpathian Journal of Earth and Environmental Sciences, 11(2), 583-598.

[23] Raja, P., Bhaskar, B. P., Surendran, U., Rajan, K., Sarkar, S. K., Malpe, D. B., & Nagaraju, M. S. S. (2018). Pedogenesis of spatially associated red and black soils in Purna valley from semi-arid region of Central India. Chemical Geology, 483, 174-190.

[24] Wang, C., McKeague, J.A. (1982). Illuviated clay in sandy podzolic soils of New Brunswick. Canadian Journal of Soil Science, 62(1): 79-89. https://doi.org/10.4141/cjss82-009.

[25] United States Department of Agriculture. (2006). Keys to soil taxonomy (10th ed.). USDA Natural Resources Conservation Service.https://www.scribd.com/doc/36962757/9070669-Keysto-Soil-Taxonomy-Tenth-Edition-2006

[26] Gee, G. W. and Bauder, J. W. (1986). Partial size analysis. In Methods of Soil Analysis Part(1): Physical and Mineralogical Methods (2nd ed.). Edited by A. Klute, PP: 383-409.

[27] Richards, L.A. (1954) : Diagnosis and improvement of saline and alkali, soils U.S. Salinity Laboratory DA, US Dept. Agro. Handbook, 60, 160p.

[28] Jackson, M. L.(1958). Soil chemical Analaysis.Prentic- Hall Inc. Engle wood, Cliffs, N.J.

[29]Page, A.L., R.H. Miller and Kenny, D.R. (1982). Method of soil andlysis part (2), 2nd ed. Agronomy series 9. Amer. Soc of Agron, Madison, Wisconsin. Potassium in Soil: Amini review. Cheni. Int. 2 (1), 58-69.

[30] Brewer , R. 1964. Fabric and mineral analysis of soils . John Wiley and Sons , Inc. , New York , London , Sydney , USA.

[31] Stoops , G. 1998. Key to the ISSS Handbook for soil thin section description . Natuurwet. Tijdschr. 78 : 193-203.

[32] Brewer, R. (1976). Fabric and mineral analysis. Soil Science, 100(1): 73.

[33] FitzPatrick, E.A. (1981). The micromorphology of soils, a manual for the preparation and description of thin sections of soils. 1980. Soil Science, 132(5): 380.

[34] Nesbitt, H. W., & Young, G. M. (1984). Prediction of some weathering trends of plutonic and volcanic rocks based on thermodynamic and kinetic considerations. Geochimica et cosmochimica acta, 48(7), 1523-1534.

[35]Harnois, J., Moore, J.M., 1988. Geochemistry and origin of the ore chemistry formations. A transported paleoregolith in the Grenville Province of Southern Ontario. Canada. Chem. Geol. 69, 267–289. https://doi.org/10.1016/0009-2541(88) 90039-3.

[36]Parker A (1970) An index of weathering for silicate rocks. Geology Magazine 107: 501-504.

[37] Roaldset, E. L. E. N. (1972). Mineralogy and geochemistry of Quaternary clays in the Numedal area, southern Norway.

[38] Souri, B., Watanabe, M.,&Sakagami, K. (2006). Contribution of Parker and Product indexes to evaluate weathering condition of Yellow Brown Forest soils in Japan. Geoderma, 130(3-4), 346-355.

ISSN 2072-3857

[39]Fedo, C. M., Wayne Nesbitt, H.,&Young, G. M. (1995). Unraveling the effects of potassium metasomatism in sedimentary rocks and paleosols, with implications for paleoweathering conditions and provenance. Geology, 23(10), 921-924.

[40]Chittleborough, D.J. (1991). Indicators of weathering for soils and palaeosols formed on silicate rocks. Australian Journal of Earth Sciences, 38(1): 115-120. https://doi.org/10.1080/08120099108727959.

[41]Darmody, R.G., Thorn, C.E., Allen, C.E. (2005). Chemical weathering and boulder mantles, Kärkevagge, Swedish Lapland. Geomorphology, 67(1-2): 159-170.https://doi.org/10.1016/j.geomorph.2004.07.011.

[42]Cox, R., Lowe, D. R.,&Cullers, R. L. (1995). The influence of sediment recycling and basement composition on evolution of mudrock chemistry in the southwestern United States. Geochimica et cosmochimica acta, 59(14), 2919-2940.

ISSN 2072-3857